WELDING RESEARCH

SUPPLEMENT TO THE *WELDING JOURNAL,* APRIL 1991

Sponsored by the American Welding Society and the Welding Research Council

Process Control of GMAW: Sensing of Metal Transfer Mode

Data acquired from visual records synchronized with electronic sensors are used to evaluate process control potentials

BY J. A. JOHNSON, N. M. CARLSON, H. B. SMARTT AND D. E. CLARK

ABSTRACT. One of the requirements of a sensing system for feedback control of gas metal arc welding (GMAW) is the capability to determine the metal-transfer mode. Because the operating boundary for the desired transfer mode, expressed as a function of mass input and heat input, may vary due to conditions beyond the control of the system, a means of detecting the transfer mode during welding is necessary. The metal-transfer mode has a large effect on weld pool behavior in GMAW, which, in turn, influences penetration, solidification, heat flow and the available range of welding positions and parameters. A series of sensing experiments was performed during which the audio emissions, welding current fluctuations and welding voltage fluctuations were recorded as a function of the transfer mode. Using laser backlighting and spectral filtering to suppress arc light, high-speed movies of the droplet formation and detachment were taken synchronously with the sensing data. The high-speed film was analyzed to investigate the physics of drop transfer. The film was synchronized with the digitized signal using an LED mounted in the camera pulsed at a set rate and recording the pulses on film and with the sensor data. A second LED was used to mark the film at the beginning of the data-acquisition period. Thus, transfer events recorded on the film can be analyzed and correlated with the digitized sensor data. Data acquired during globular transfer, spray transfer and stiff spray or streaming transfer were observed to correlate with droplet detachment and arc shorting. Instabilities in the transfer mode and mechanisms of drop detachment affecting drop velocity are discussed. Although the current and voltage data are also dependent on the characteristics of the welding power supply, the audio, current and voltage data could be used to discriminate among these different transfer modes.

KEY WORDS

GMAW Process Control
Metal Transfer Mode
Transfer Mode Sensing
Sensing Experiments
High-Speed Movies
Droplet Formation
Current/Voltage Data
Feedback Control
Streaming Transfer
Globular/Spray Transfer

J. A. JOHNSON, N. M. CARLSON, H. B. SMARTT and D. E. CLARK are with Idaho National Engineering Laboratory, EG&G Idaho, Inc., Idaho Falls, Idaho.

Introduction

In the GMAW process, a welding arc is struck between the workpiece and the tip of a consumable wire electrode. The electrode carries the welding current, sustaining the arc. The electrode melts, resulting in the detachment of metal droplets which supply filler metal to the joint (Ref. 1). The mode of metal transfer depends on the various welding parameters. The transfer mode in gas metal arc welding (GMAW) is an important influence on weld quality. In particular, in welding automation, process stability may depend not only on commonly measured parameters such as DC voltage and current, but also on the transfer mode.

In general, a spray transfer mode operates at higher average currents than a globular mode, and is more suitable for flat welding of thick-section metals. Dur-

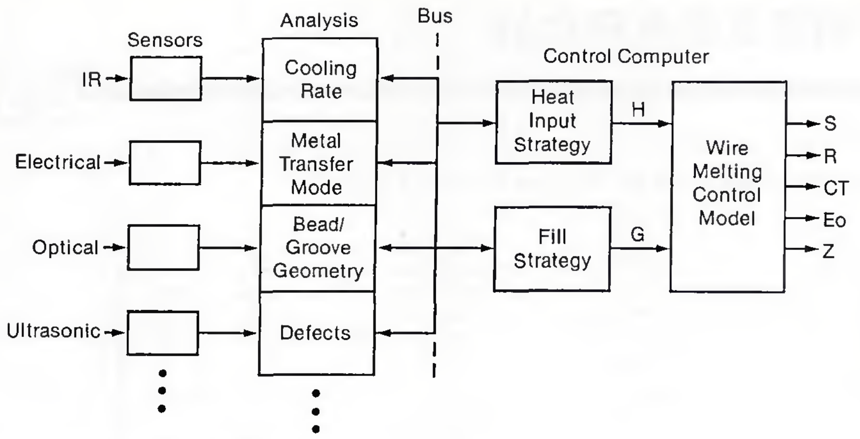

Fig. 1 — Schematic for feedback control of GMAW.

ing an automated welding process, as welding gun position or stand-off distance changes, the transfer mode may change inadvertently, altering weld shape, penetration and quality. Thus, beyond the current practice of designing welding parameters to lie in a stable transfer region, it may be desirable to detect and deliberately control transfer modes.

Research in welding at the Idaho National Engineering Laboratory (INEL) is currently concentrating on the development of sensing, modeling and control schemes for GMAW (Refs. 2,3). For process control of GMAW, various types of sensors can be used to measure properties of the GMAW process and provide input to the system. A diagram of an automated welding control scheme is shown in Fig. 1. On the left are various types of sensors capable of detecting characteristics of the weld process. These sensors may be categorized according to type, such as infrared, electrical, optical and ultrasonic, or according to the properties of the welding process. They measure such things as weld pool geometry (optical and ultrasonic), cooling rate (infrared), discontinuities (ultrasonic) and droplet transfer mode (electrical).

Optical techniques can be used for joint tracking and fitup measurements, as well as for observing the shape and size of the top surface of the molten weld pool and the droplet detachment (Ref. 4). Richardson at Ohio State University has developed a vision system that views the pool through a special hollow welding gun body, providing some of the information similar to that provided by a vision system developed at INEL (Ref. 5). Ultrasonic methods are also being used to determine the pool geometry at the molten/solid interface (Ref. 6). Initial experiments were performed by Lott (Ref. 7) at INEL and Katz and Hardt at MIT (Ref. 8). Fenn and coworkers at Brunel University claim to have used ultrasonic measurements to determine the depth of penetration and to control the depth by varying the welding current in submerged arc welding (Ref. 9). Unfortunately, insufficient detail was presented in their papers to confirm or repeat their results.

Infrared sensors can be used to detect cooling rate, which is important for control of fracture toughness while maintaining strength in some steels (Ref. 10). Workers at Auburn University are also using infrared techniques for determining weld pool size and tracking measurement and process control (Refs. 11,12).

Ultrasonic sensors can be used to detect discontinuities in the weld during welding. The ultrasonic echoes from the molten/solid interface and the molten pool provide information about the quality of the fusion zone and the geometry of the molten pool. Unacceptable welding conditions that can result in porosity, incomplete sidewall penetration or undercut are detected (Ref. 13).

This paper addresses the electrical sensor in Fig. 1, which monitors variations in current and voltage that are superposed on the nominal DC values and the drop transfer mechanisms as they correlate to film and digitized data. The analysis provides information on the transfer mode of droplets detaching from the melting wire (Refs. 14–16). This is important since for many applications a particular transfer mode (Ref. 17) is required for quality welds and the boundary between this transfer mode and other, undesirable modes may shift due to factors beyond the control of the system.

Other sensors may also be used that are not listed on the control-scheme diagram. These include spectroscopic and photometric measurements of the arc for penetration control (Ref. 18), real-time radiography for detection of discontinuities (Ref. 19), and measurements of the audible sound emitted by the process for droplet transfer mode detection (Ref. 15).

The column labeled Analysis in Fig. 1 is where the raw sensor data are converted into the desired information on the process, such as cooling rate deduced from the raw infrared data. This information is passed on to two intelligent modules which use the information to determine the best method of filling the weld while maintaining the correct heat input to the weld. These modules contain economic as well as physical constraints since the fill strategy determines the number of passes required to fill the joint and thus the productivity of the process.

The final step is a model of the welding process which converts the requested heat and fill inputs to the physical welding parameters (Ref. 20). Both Hardt (Ref. 21) and Eagar (Ref. 22) at MIT are working on aspects of modeling GMAW, including the control scheme required for a nonlinear, cross-coupled system and the physical aspects of the wire melting.

This paper describes the acquisition and analysis of electrical and high-speed film data and the correlation of that data to the detection of droplet transfer mode as a potential method of controlling the transfer mode. A series of experiments was performed using three different methods to sense the metal-transfer mode dynamically. Airborne audio emissions, welding

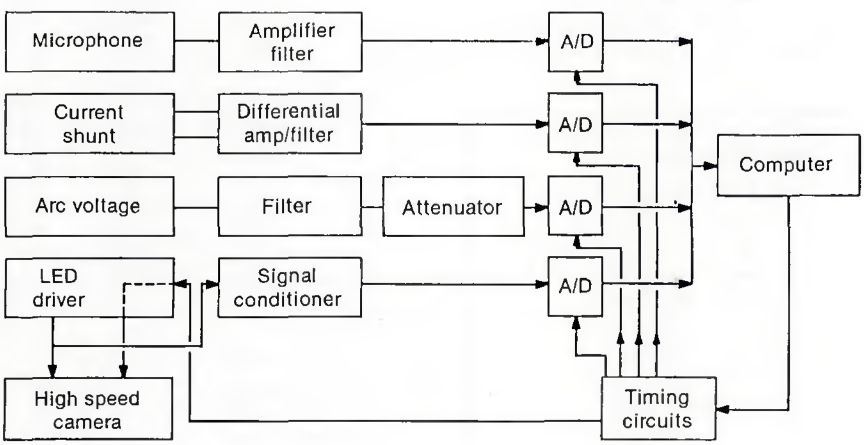

Fig. 2 — Schematic for sensor data acquisition.

current fluctuations and voltage fluctuations were recorded as a function of the transfer mode. To correlate sensor data with the actual transfer mode, high-speed movies of the droplet transfer were acquired synchronously with the sensing data.

Experimental Procedure

The gas metal arc welding process was observed by a laser backlighting technique to suppress the arc light (Ref. 23). A collimated, 25 mW He-Ne laser beam was passed through the space between the weld head and workpiece, through a laser line filter and the appropriate neutral density filters, and into a Hycam high-speed 16-mm camera. A size reference standard was included in the frame near the welding site for later calibration of measurements (Refs. 24, 25).

All welds were made with a standard water-cooled welding gun, using 0.89-mm (0.035-in.) diameter E70S-3 carbon steel wire and Ar-2%O_2 shielding gas. The workpiece was moved under the welding gun at a travel speed of 4.2 mm/s (10 in./min) to make bead-on-plate welds. Direct current levels between 150 and 240 A were examined, at operating voltages of 25 to 29 V. Lower current levels within this range produced a globular transfer, while higher current levels produced a spray or streaming transfer. Contact tube-to-work distances were varied between 15.9 to 22.2 mm (0.625 and 0.875 in.). Two welding power supplies were used, a conventional three-phase transformer-rectifier (Linde SVI-300) and a transistor power supply capable of pulsed output (Philips PZ-2351).

The current and, therefore, the transfer mode were changed by changing the wire feed speed. At low wire feed rates, the current was low and the drops were generally larger than the wire diameter, corresponding to globular transfer. At intermediate wire feed rates the droplets were generally smaller than the wire diameter, corresponding to spray transfer. At high rates, a stream of liquid formed at the end of the wire, which broke up into many small droplets before reaching the weld pool. This mode is called streaming or "stiff spray transfer."

A simplified schematic of the data-acquisition system is shown in Fig. 2. A portable workstation (Ref. 26) based on a MicroVax II computer and a Computer Automated Measurement and Control crate (CAMAC, IEEE-583 Standard) were used for data acquisition. Three channels of sensor data were acquired along with a fourth channel that recorded signals used to synchronize the sensor data with individual frames on the film taken with a high-speed camera.

The sensors were a Shure 5775 microphone mounted 330 mm (13 in.) from the weld pool, a current sensor and a voltage sensor. The signal from the microphone was amplified over a bandwidth from 10 Hz to 30 kHz. The bandwidth of the microphone was not measured. A shunt in the ground cable from the weld sample to the power supply was used to measure the welding current. The voltage across the shunt was amplified by a differential amplifier with a bandwidth from 10 Hz to 30 kHz. Thus, the DC portion of the welding current was not acquired, only fluctuations about the average DC value within the bandwidth of the amplifier. The voltage signal was obtained from leads connected to the contact tube and the ground on the workpiece, filtered to a bandwidth from 10 Hz to 30 kHz so that only the AC component of the signal was digitized. (The DC parts of the current and voltage were recorded on a strip chart recorder.)

The four channels were digitized at a synchronous 50-kHz rate. A maximum of 8192 points can be stored in each digitizer. At these sampling rates, 163.8 ms of data can be acquired on each channel. Data acquisition began when a signal was sent to a buffer that triggered all four digitizers.

The fourth channel acquired the analog pulses from a multichannel light-emitting diode (LED) driver for the high-speed camera so that the sensor data can be correlated with the film data. These pulses were sent to the camera at a set repetition rate where they triggered an LED, which then placed a mark that can be seen in the margin of the film. The control box was designed so that a double mark was placed on the film every 10 cycles and a triple mark every 100 cycles. These double and triple pulses were also recorded by the digitizing system to allow correlation between the film and the digitized data. The LED film marker pulse sent from the control box to the fourth channel was pulse stretched to ensure that the pulse width was sufficient to be digitized. Knowing that the film LED marks occurred five frames prior to that frame passing the shutter of the camera, the digitized data can be correlated to the film data within a frame (0.18–0.20 ms) of the actual occurrence of an event. In addition, a pulse was sent to the film control box from the workstation to trigger a second LED, which marks the film at the beginning of the data-acquisition cycle.

Films were measured frame by frame on a film analyzer, which allowed the measurement of transfer events, including electrode extension, drop diameter and frequency, and drop velocity and acceleration. Higher speed films, at 5000–5500 frames/s, were used for drop-detachment and acceleration studies, while slower speed films, at 500 frames/s, were used for longer sample times to determine transfer mode stability and behavior.

Although the shutter speed of the camera at 5000–5500 frames/s was high enough to give drop images unblurred by motion, individual in-flight drop measurements often showed considerable scatter, so groups of 20 drops were measured and their positions vs. time were averaged. Statistical analysis suggested that this number of drops was more than adequate to give high confidence in the velocity and acceleration values thus obtained.

Experiments with a Transistor Power Supply

The Philips transistor power supply (Model PZ 2351/60) was used in the experiments described in this section. It achieves its precise DC pulse capabilities by pulse width modulation at 40 kHz. For these experiments, the supply was operated in the constant voltage mode. The voltage setting, the wire feed speed and the torch-to-workpiece distance determined the current and the droplet transfer mode.

Data were acquired in the following manner. The welding operator established a steady arc in the desired transfer mode. At the operator's signal, the high-speed camera was turned on and the data-acquisition system armed. After a programmed delay of up to 3 s to allow the film to accelerate to the final speed of 5000 to 5500 frames/s or 500 frames/s, the acquisition system acquired a set of data on all four channels simultaneously and also sent pulses to the second LED to mark initiation of data acquisition on the film as described above. At the termination of data acquisition, the digitized information was written to a disk for later analysis and plotting. Although each digitized data set acquired only 8192 points of data, 15 data sets (approximately 2000 ms, or 2.0 s of data) were acquired between the two filming rates. Digitized data were also acquired without acquiring high-speed film to determine that the desired transfer mode was being achieved. The time intervals of the digitized data acquired in these data sets provided several additional seconds of digitized data. Based on the number of data sets acquired and analyzed and the consistent trends observed for each transfer mode, the data and results to be presented are predictive of the mode of metal transfer.

Electrical data were acquired for three different transfer modes: globular, spray and streaming. The three modes of metal transfer were achieved by using nominal welding parameters listed in Table 1. Figure 3 presents photos made from camera frames acquired synchronously with the digitized data for three transfer modes. In globular transfer (Fig. 3A), large droplets of diameters in excess of the diameter of the electrode detached as discrete drops at a rate of up to 100/s. In spray transfer (Fig. 3B), small droplets of metal detached from

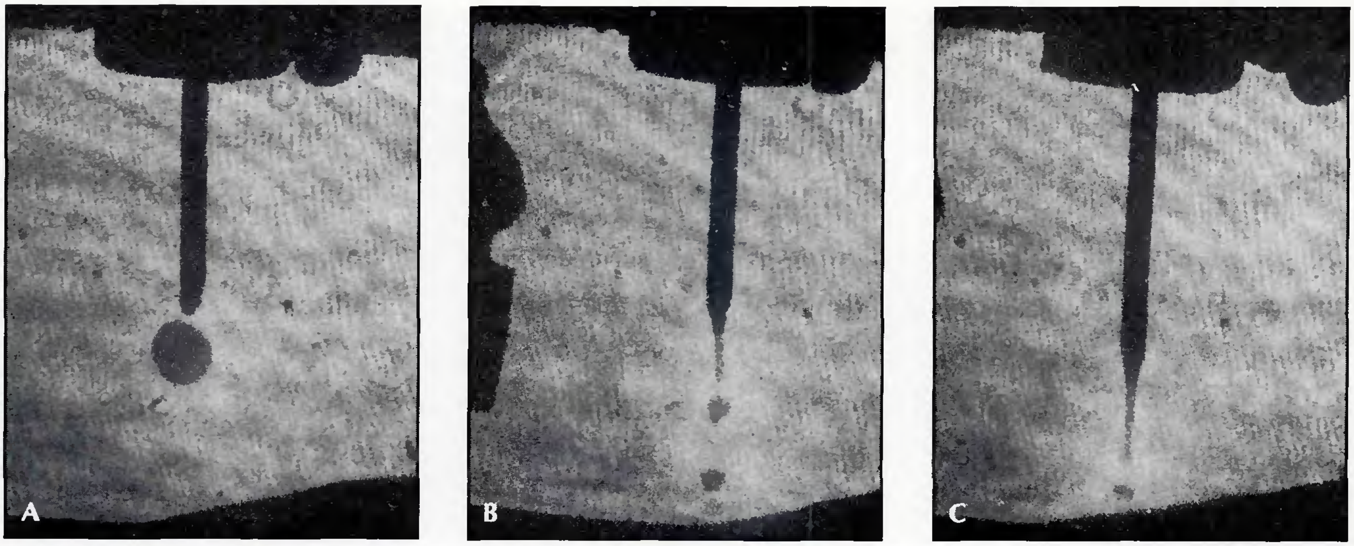

Fig. 3 — Three metal transfer modes. A — Globular; B — spray; C — streaming.

the electrode at a rate of several hundred per second. In streaming transfer (Fig. 3C), small droplets detached from a liquid column of metal attached to the electrode (Ref. 1). The necessity for sensing and process control is evident in Fig. 3B. Although welding parameters were set for spray transfer, notice that a short liquid column extends beneath the electrode indicating that the process was transitioning from spray transfer, the desired transfer mode, to streaming transfer. This transition mode will be discussed in more detail in the drop transfer mechanisms section of the paper.

A 40-ms portion of the 160 ms of acquired digitized data taken during globular transfer is shown in Fig. 4A. Pulses in the "Camera Sync" plot occurred at 1-ms intervals and are the record of the times that the LED marks were placed on the film. Note that every tenth pulse was doubled and that this particular data set included a triple mark, which occurred every 100 ms. In addition, using these pulse marks allowed a correlation between droplet detachments on the film and signals in the three sensor channels to be made with a precision of one frame of film (0.2 ms at 5000 frames/s and 2.0 ms at 500 frames/s).

The voltage and current data have two obvious features in Fig. 4A at 50 and 75 ms. The beginning of each of these features correlates precisely to a large globular droplet detaching from the end of the wire. This was determined by correlating the synchronizing signal recorded with the sensor data with the LED marks in the margin of the film. Not quite so obvious are two features in the audio signal that occurred about 1 ms after the current and voltage features. This signal, delayed by 1 ms, correlates to the time required for sound to travel the 330 mm (13 in.) from the tip of the wire to the microphone after the droplet detachment. Thus, this audio signal correlates to the same physical event that caused the excursions in the electrical signals; the droplet detachment.

The data for current do not show the sharp features observed in the voltage data. This was probably due to the inductance of the cable, which limited the bandwidth of this sensor. Estimates of the inductance and resistance of the system indicated that the time constant of the system was about 0.2 ms, corresponding to a bandwidth of 5 kHz.

The entire 160-ms data set for the audio, current and voltage for this experiment in globular transfer mode is shown in Fig. 4B. A total of nine features is seen in the entire data set, and each corresponds to a droplet detachment observed on the expected frame on the film. Based on the 160-ms data set, approximately 50–60 globular drops would detach in a 1-s interval. An important point is that the interval between detachments was not regular, and varied according to the size of the drop. This is discussed in more detail below and in Ref. 27.

In addition, at the start of the data set the positive-going portion of a voltage fluctuation cycle was observed due to an additional drop, which detached just a few frames before the acquisition system began to record data. The audio signal was more difficult to correlate on this compressed scale. However, for eight of the nine droplet detachments (and for the detachment at the beginning, which was observed in the audio data because of the 1-ms delay), a feature similar to those in Fig. 4A was observed. The exception was for the detachment at 138 ms where no correlating signal was observed in the audio channel.

Data for two additional modes of droplet transfer — spray and streaming transfer — were acquired. Figures 4C and 4D show results analogous to Fig. 4B for spray and streaming transfer, respectively. For spray transfer, features similar to those observed for globular transfer were observed unambiguously in the current and voltage data — Fig. 4C. Each of these features again correlated with a droplet detachment, observed on the corresponding frame of film. The features were smaller in amplitude relative to the 40-kHz noise of the power supply and occurred more often, corresponding to the smaller droplet size and the greater rate of droplet detachment. The droplets detached at an average rate of 560 Hz as calculated from a 32-ms period during which 18 droplets detached. Between about 18 and 26 ms, the transfer mode changed and numerous small droplets detached. Following this period, the droplets again returned to the normal size for spray transfer.

In streaming transfer, little fluctuation was observed in the digitized data on the three channels — Fig. 4D. This correlated with the lack of a well-defined detachment in this transfer mode since a nearly continuous stream of liquid melted off the wire, only breaking up after traveling downward some distance. Although transfer can occur when the liquid column contacts the weld pool, 29 distinct drop-

Table 1—Welding Parameters(a)

Transfer Mode	Volts	Amperes	Wire feed Speed (mm/s)	(in./s)
Globular	25.6	173	130	5.1
Spray	27.0	234	190	7.5
Streaming	26.7	275	250	9.8

(a) Contact tube-to-workpiece distance 15.9 mm (0.63 in.).
Travel speed 4.2 mm/s (9.9 in./min).
Cover gas 98% Ar, 2% O_2.
Electrode type: E70S-3.
Electrode diameter: 0.889 mm (0.035 in.).

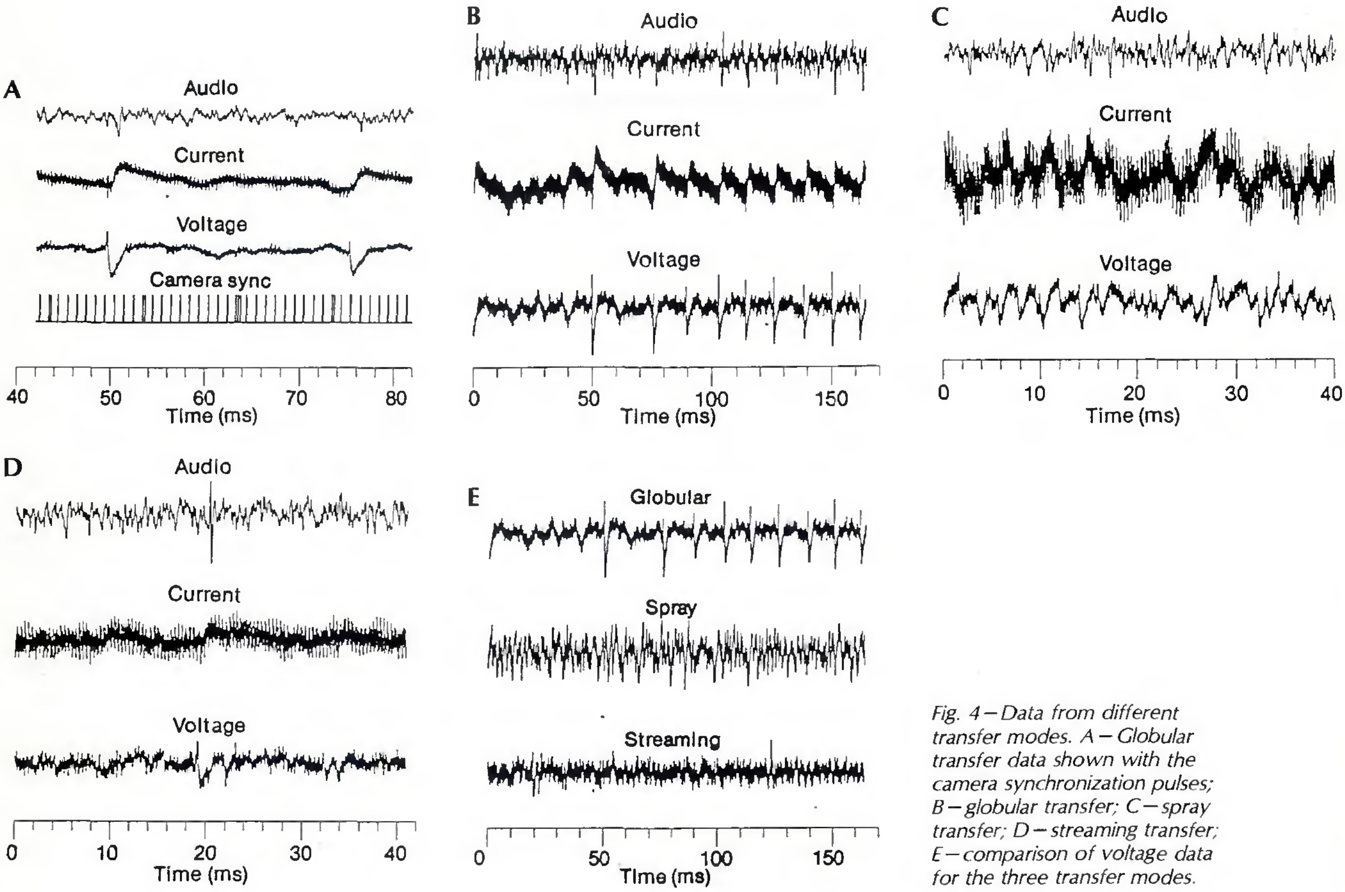

Fig. 4 — Data from different transfer modes. A — Globular transfer data shown with the camera synchronization pulses; B — globular transfer; C — spray transfer; D — streaming transfer; E — comparison of voltage data for the three transfer modes.

lets were observed in a 40-ms period, which calculates to 700–750 drops/s. One feature of significance occurred at about 19 ms and may correlate with the steam bridging the gap between the end of the wire and the weld pool, causing a short. Unfortunately, this could not be directly confirmed from the film since it was difficult to identify the rapid shorting of the liquid column on the film even at the 5000–5500 frame/s rate.

In Fig. 4E, the voltage data for the three modes of transfer are compared. The amplitudes of the features were seen to decrease and the frequency to increase as the size of the droplets decreased and frequency of detachment increased going from globular to spray mode. In streaming transfer, it was difficult or impossible to detect individual droplets. An expert system could be used to detect and discriminate among the transfer modes in real time. Adams and Siewert have also addressed this possibility (Ref. 16). Some features the system could use for discrimination of the three transfer modes are the peak amplitude of voltage signals and the time interval between the peaks. The output of a counter and two discriminators would contain the needed information about the average rate of droplet detachment and the size of the droplet. Rules could be established to use this information to determine the transfer mode. The expert system could then provide metal transfer input information to the feedback system for control of the welding process (Refs. 16, 28).

Experiments with a Transformer-Rectifier Power Supply

Data acquisition with the sensing system was also conducted using a Linde (Model SVI-300) power supply. In this supply, the three-phase, 60-Hz power was transformed and rectified to produce the desired DC voltage. This resulted in a rather large 360-Hz noise ripple in the audio, current and voltage signals. Band-stop filters at 360 Hz were placed in the circuits connecting the audio and voltage sensors to the digitizers. The current signal was deliberately not filtered at 360 Hz to determine if the ripple had any effect on the droplet detachment discussed in a later section of this paper (Ref. 24). The need for mode detection capability was dramatically demonstrated during these experiments since several data sets were acquired with welding parameters that normally resulted in globular transfer, but the transfer mode was determined to be spray transfer when the droplet size was observed on the film.

In Fig. 5, the results for globular transfer using the transformer-rectifier power supply are shown. The data are not as easily interpreted as those for the transistor power supply due to electrical noise. The problem of electrical noise in data interpretation was also noted by Kohn and Siewert (Ref. 29). However, each of the two bipolar spikes in the voltage data correlated to the two globular droplet detachments observed on the film during this time. The current data (not filtered at 360 Hz) showed just the 360-Hz ripple with 120-Hz subharmonic. The audio signal was also uninformative due to the presence of a large amount of electrical interference. According to welders, the sound that they heard for each mode was independent of the type of power supply, indicating that if the electrical interference were eliminated, the droplet detachments could be distinguished in the audio signal.

Interpretation of the spray data acquired using the transformer-rectifier power supply was more difficult. A correlation between the larger spray droplet detachments and a voltage fluctuation was observed. As the droplet size decreased so did the amplitude of the fluctuation of the voltage digitized at the time of droplet detachment. Small droplet detachments were not observed in the voltage. The audio and current data were not used for interpretation for reasons previ-

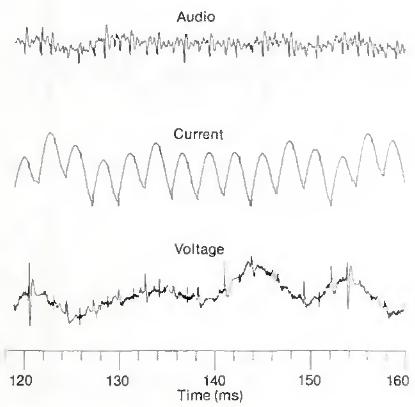

Fig. 5 — Globular transfer data acquired while using a transformer power supply.

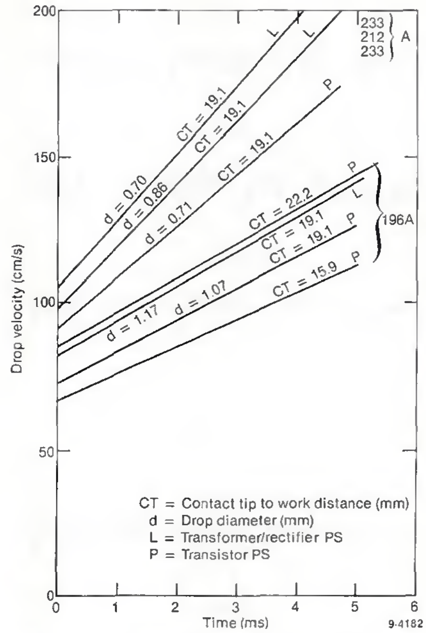

Fig. 6 — Drop velocity with time for GMAW, 0.035-in. wire, Ar-2%O_2 shielding gas.

ously stated in this section.

No data were acquired in the streaming mode with the rectifier power supply.

Power Supply Variations

Comparison of the transistor and rectifier power supply data revealed that the mode of droplet transfer could be detected for either supply. However, the detection did require knowledge of the baseline signature of each power supply. In the globular mode of transfer for both supplies, the droplet detachments produced a distinct, large amplitude, low-frequency fluctuation in both the voltage and current. When spray droplets detach, the frequency of fluctuations in current and voltage increased, and the amplitude of the fluctuations decreased compared to globular transfer. Detection of spray transfer depended on the droplet size. As the size of the spray droplets decreased, so did the ability to detect detachment of the individual droplets. In the extreme case of the streaming transfer mode, few fluctuations in the voltage and current data were observed. The fact that each mode of droplet transfer had a unique voltage signature in the acquired digitized data for both supplies demonstrated the feasibility of using voltage sensing to determine droplet transfer modes.

However, signatures of the different modes were not the same for the two power supplies, thus presenting some difficulty in introducing a generic system for all power supplies. Interpretation of the acquired current and voltage signals was based on knowledge of the power supply baseline signature and the change in that signature during droplet transfer. Since welders are capable of using the audio information they heard to determine the transfer mode, independent of the power supply, some salient characteristics of the audio signal must be independent of the power supply. However, information from the audio sensor must be improved by decreasing the extraneous noise and enhancing the data feature associated with the droplet transfer. This would require improved microphones, electronics and filtering for the audio channel. Several possibilities for improving the audio signal include using correlated signals from two microphones at equal distances from the welding gun or using a parabolic reflector focused on the welding gun to improve the signal-to-noise ratio.

Drop Transfer Mechanisms

To better understand the drop transfer mechanisms involved in GMAW, the high-speed film acquired from the two power supplies (Linde labeled L and Philips labeled P in Fig. 6) was analyzed to determine those mechanisms. Initial measurements of drop frequency from film acquired using the Linde power supply suggested that there might be a variation in drop transfer rate at approximately 60 Hz. If the droplet tends to be ejected at a particular point in the ripple waveform, rather than at other random times, then the droplet transfer rate would tend to cluster around the ripple frequency, an expected 360 Hz in this case. A 60-Hz rate, being an even divisor of 360 Hz, might be the result of asymmetrical rectification or another electrical effect. For this reason, the correlation of droplet detachment with the power supply ripple was examined more closely. The power supply ripple was approximately 18 A, something less than 10% of the welding current. The correlation of this ripple with drop detachment events proved to be negative as drop detachment occurred at various, apparently random, places with respect to the ripple. Evidently, this degree of current ripple does not affect transfer events in the range of welding parameters examined, and the apparent 60-Hz variation in drop frequency may be due to other, as-yet undetermined, factors.

Figure 6 shows the drop velocity with time for a number of welding conditions. It can be seen that the higher currents (212 to 233 A) produce smaller drops than those produced by the lower current (196 A). The accelerations of these smaller drops were also higher, averaging around 20,000 cm/s^2, vs. about 11,000 cm/s^2 for the larger drops. Increasing the electrode extension in the lower current welds appeared to increase both the initial velocity and the acceleration of the drops slightly, although no obvious affect on drop size was observed. Finally, at identical measured operating conditions, the transistor power supply appeared to produce somewhat lower initial velocities and lower accelerations, as compared with the transformer-rectifier power supply, although it is not clear at this point why this should be so.

Drop acceleration after detachment has been ascribed to aerodynamic drag within the plasma, due to the strong electromagnetically driven gas flow from electrode to workpiece. Figure 7 shows typical results for the drops observed here with theoretical curves derived from the aerodynamics by Lancaster (Ref. 30). It can be seen that the agreement between theory and the present experimental results was reasonably good, suggesting that, in fact, aerodynamic forces were responsible for drop acceleration after detachment.

The drop also had an initial velocity at separation, as indicated by the fact that the intercepts at time zero in Fig. 6 lie at 70–100 cm/s. The wire speed for these welds was 15–20 cm/s, leaving a deficit of 50–80 cm/s to be accounted for. It is not the purpose of this work to examine drop formation and detachment mechanisms in detail, but we may consider the relevance of some of the postulated detachment mechanisms (Ref. 30).

The static force balance theory balances the surface tension, electromagnetic, aerodynamic drag and gravitational forces on a drop. Acceleration of the drop after detachment would then be due to the applicable manifestations of these same forces. The columnar instability mechanism states that pressure imbalances due to perturbations shorter than a critical wavelength will be unstable and break a liquid column into drops. The application of the Lancaster model involves uncertainties; however, the initial velocity and acceleration associated with this process corresponds to observed velocities, as well as the further acceleration by other forces identified in the static force balance theory. At lower currents, with larger (globular) drops, the static force balance theory (or a modification of it for tapered electrodes) can account for drop transfer, while at higher currents (typically above 200 A), a columnar instability mechanism may be responsible for the transition to spray transfer with its smaller drops.

This work was near the transition current between globular and spray transfer. It is currently of some interest just how abrupt this transition may, in fact, be, and these results may shed some light on this.

Regardless of how the instability leading to detachment is formed, at the instant of detachment the drop is 1) free of the surface tension force binding it to the electrode, 2) subject to the pressure forces and the aerodynamic drag that will soon be responsible for accelerating it through the arc column, 3) subject to an uncertain amount of electromagnetic force, depending on the local current paths, and 4) subject to the gravitational force.

The "teardrop" shape of the drop at the instant of detachment is not an equilibrium shape, and an imbalance of surface tension energy can be visualized in Fig. 8, where the drop is divided into a cone and a hemisphere. Film evidence shows that this elongated shape very rapidly disappears within the space of one or two frames at 5500 frames/s, or 0.2–0.4 ms. The forces maintaining the elongated shape store energy in the form of this unbalanced surface tension, which is then released, analogous mechanically to shooting a rubber band. In most films, longitudinal oscillation of the drop before detachment is seen, an observation consistent with, although not unique to, such a model.

Table 2 shows the results of two calculations attempting to quantify this stored energy. In the energy calculation, the surface energy difference, balanced around the drop's centroid, was assumed to be entirely transformed into translational kinetic energy; this was, of course, an ideal case, since the stored energy may also emerge as rotational or oscillatory kinetic energy, internal heating or in other forms. The value for surface tension used was a handbook value (Ref. 31) of 1500 ergs/cm^2 (for iron), which might be quite different in the actual plasma environment. In the momentum calculation, the momentum was derived from the transport of the mass of the upper part of the drop toward the centroid of the drop in the upper limit of the time permitted by the film evidence (0.0004 s), and was hence a more conservative calculation. One of the uncertainties in this calculation was that fluid flow, shape changes and asymmetries with respect to the arc column, not readily accessible to measurement by film techniques, might alter the starting assumption.

The quantities shown in Table 2 are in approximate agreement with the gap between wire feed speed and the initial velocities observed in the films, *i.e.*, 50–80 cm/s, particularly for the larger cone heights, which are, in fact, closer to the observed transfer geometries. It should be emphasized that this calculation is not a substitute for the more fundamental columnar instability or force balance models, but a model of an experimentally observed starting point for the drop's departure from the end of the wire.

In a weld at 160 A observed at 500 frames/s, where the expected transfer mode was globular, episodes, separated by a period of about a second, of spray transfer that we call a "mixed mode" transfer, were observed. The typical course of events involves 1) typical globular transfer with drop diameters at or exceeding the wire diameter, 2) the retention of one of these drops for a considerably longer time, during which it grows to two or more times the wire diameter and the electrode extension increases, and 3) the transfer of this large drop, followed by a stream of much smaller drops typical of higher current spray transfer, entailing a rapid decrease in electrode extension (Ref. 27).

Although the consistency or extent of this phenomenon have not yet been determined, and electrical and acoustic data have not been acquired while it is happening, it is interesting in several ways. Recent work suggests that the transition between globular and spray transfer is fairly continuous, and that a number of variables in current path, the nature and origin of the electrode taper, and the thermal properties of the developing drop, complicate the drop stability picture (Ref. 22). Under the proper conditions, it may be that a continuous change from globular to spray transfer (*i.e.*, a continuous decrease in drop size and increase in frequency) does not occur. Instead, as the current approaches the nominal transition point, increasingly frequent groups of drops transfer in a spray mode, until, eventually, a pure spray mode exists. A similar instability was noted by Halmoy (Ref. 32) at similar welding parameters (1.2 vs. 0.89 mm wire, 102.7 vs. 110 mm/s wire feed speed, and 25 vs. 15.9 mm electrode extension), and was ascribed to the negative slope of the current-voltage characteristic of the arc below 200 A, and related to the transit time across the electrode extension. This work may be an observation of the same phenomenon, although Halmoy's descriptions of events differ from these observations. These differences might be resolved by further work, including voltage and current measurements during filming.

In terms of the filmed behavior, a key issue is why the drop before the spray transfer episode becomes so large, and why a globular regime reestablishes itself afterward. By definition, drop velocity was less than the wire velocity when the drop was growing, and greater when the drop transfered. Other factors, however, must be adjusted before a stable spray can be achieved. As the wire feed speed is increased into the spray range, electrode taper must develop and the thermal and force balance conditions for spray

Table 2—Calculated Initial Velocities Due to Stored Energy in the Drop at the Instant of Detachment (drop radius = 0.076 cm)

Cone Height (cm)	Energy Calculation (cm/s)	Momentum Calculation (cm/s)
0.16	35.9	1.3
0.18	45.8	5.5
0.20	53.2	11.1
0.25	66.2	29.0
0.30	75.0	51.5

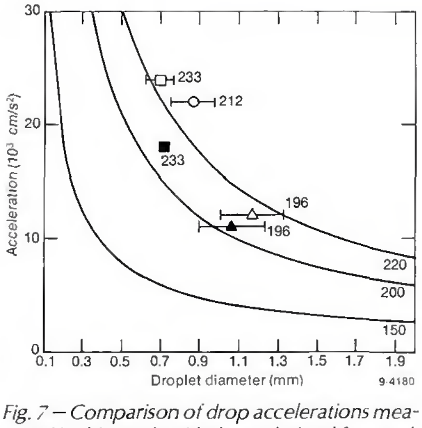

Fig. 7 — Comparison of drop accelerations measured in this work with those derived from calculated plasma velocities by Lancaster. Currents in amperes.

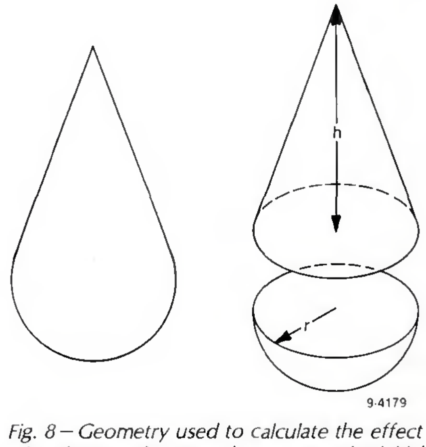

Fig. 8 — Geometry used to calculate the effect of surface-tension-stored energy on the initial velocity of the drop.

transfer must be achieved. The increased wire feed speed may at first lead to increased electrode extension, and when the large drop finally transfers, the system finds itself at an abnormally high electrode extension with a very small amount of melted material on the end of the electrode; the melting rate increases, spray transfer is initiated, and the electrode extension returns to normal. At the same time, the arc length is rapidly changing, and the aerodynamic drag forces can be expected to change both as a result of this and because of the departure of the large drop, and this will strongly alter the static force balance, which partly governs transfer.

Transfer in this parameter range may thus be regulated by a complex thermal, electromagnetic and mechanical system. In certain ranges, stable globular transfer occurs; in others, stable spray transfer occurs; at certain critical parameters the melting rate instability due to arc characteristics observed by Halmoy may occur; and in still other regimes, hysteresis and even chaotic influences may apply.

Conclusions

By monitoring current and voltage of the power supply, the metal-transfer mode may be detected and the results may be used for process control of GMAW. The ability to sense the metal-transfer mode is vital to ensure that the welding machine operates in the required transfer mode to achieve the desired heat and mass input for the weld. The audio and acoustic emission sensors need to be reexamined and replaced with sensors with a more appropriate bandwidth and sensitivity for the application. The voltage and current data appear to be power supply dependent, based on the work completed with two power supplies used for these experiments. This dependence may present a potential problem in analysis of the incoming signals in the closed-loop control system because of the difference in signatures from each power supply. Drop transfer does not seem to be correlated with the 10% (18 A) ripple of a transformer-rectifier power supply. By the use of improved audio data, a power-supply-independent method of overcoming this problem may be achieved.

If only current and voltage are monitored, the input to the computer can be designed to be transparent to the user and thus more acceptable in industry. The sensors are simply monitoring the analog output normally generated by the power supply and add no additional problems in any welding application. Because the approach is capable of monitoring droplet detachment dynamically, the desired transfer mode can be sensed and controlled throughout the entire welding pass by a closed-loop control system.

These tests have demonstrated the ability to detect the detachment of individual droplets and to distinguish among three metal-transfer modes in GMAW, as well as the mechanism of droplet transfer. The acceleration of drops across the arc in globular and spray transfer modes corresponds to theoretical calculations of aerodynamic drag based on the expected gas velocities in the plasma column. The initial velocity of a drop as it leaves the wire can be accounted for by wire velocity and by both the stored surface tension energy and the observed imparted momentum in a longitudinally asymmetrical drop created by static forces at the electrode tip. During nominally globular transfer, episodes of spray transfer also periodically occur. This mixed mode suggests that the dynamics of mode changes are complex and that the mode change from globular to spray transfer may occur episodically rather than continuously.

By using the electrical sensing data combined with the knowledge of the drop transfer mechanisms, an approach capable of sensing droplet detachment in pulsed welding may be present. The detection of droplet transfer would assure that a single droplet is detached at each pulse. This would aid greatly in controlling the heat and mass input for pulsed welding and provide input data about the mode of metal transfer to a closed-loop process control system with feedback control.

Acknowledgments

This work was supported by the U.S. Department of Energy, Office of Energy Research, Office of Basic Energy Sciences under DOE Contract No. DE-AC07-76ID01570. Technical assistance was provided by U. S. Wallace, C. L. Shull and A. L. Jones.

References

1. American Welding Society, *Welding Handbook, 8th ed., Vol. 1, Welding Technology*, Miami, Fla., 1987, pp. 4–8.

2. Smartt, H. 8., Einerson, C. J., and Watkins, A. D. Modeling and Control of Gas Metal Arc Welding. Submitted to the *Welding Journal.*

3. Smartt, H. B., Einerson, C. J., and Watkins, A. D. 1988. Computer control of gas metal arc welding. *Second International Conference on Computer Technology in Welding*, The Welding Institute, Cambridge, U.K.

4. Johnson, J. A., *et al.* 1986. Automated welding process sensing and control. *Proceedings of the Second International Symposium on the Nondestructive Characterization of Materials*, pp. 409–417.

5. Richardson, R. W., Gutow, D. A., Anderson, R. A., and Farson, D. A. 1984. Coaxial arc weld pool monitoring for process monitoring and control. *Welding Journal* 63(3):43–45.

6. Carlson, N. M., and Johnson, J. A. 1988. Ultrasonic sensing of weld pool penetration. *Welding Journal* 67(11):239-s to 246-s.

7. Lott, L. A. 1984. Ultrasonic detection of molten/solid interfaces of weld pools, *Materials Evaluation* 42, p. 337.

8. Hardt, D. E., and Katz, J. M. 1984. Ultrasonic measurement of weld penetration. *Welding Journal* 63(9):273-s to 281-s.

9. Stroud, R. R., and Fenn, R. 1985. The measurement and control of penetration during submerged arc welding. *Welding Journal* 64, pp. 18–22.

10. Lukens, W. E., and Morris, R. A. 1982. Infrared temperature sensing of cooling rates for arc welding control. *Welding Journal* 61(1):27–33.

11. Govardhan, S. M., and Chin, B. A. 1989. Monitoring GTA weld puddle geometry using measured surface temperature gradients. *Proceedings of the Second International Conference on Trends in Welding Research*, Gatlinburg, Tenn., pp. 383–386.

12. Nagarajan, S., Groom, K. N., and Chin, B. A. 1989. Infrared sensors for seam tracking in GTAW. *Proceedings of the Second International Conference on Trends in Welding Research*, Gatlinburg, Tenn., pp. 951–955.

13. Carlson, N. M., Johnson, J. A., and Kunerth, D. C. 1990. Control of GMAW: detection of discontinuities in the weld pool. *Welding Journal* 69(7):256-s to 263-s.

14. Liu, S., and Siewert, T. A. 1989. Metal transfer in gas metal arc welding: droplet rate. *Welding Journal* 68(2):52-s to 58-s.

15. Johnson, J. A., Carlson, N. M., and Smartt, H. 8. 1989. Detection of metal-transfer mode in GMAW. *Proceedings of the Second International Conference on Trends in Welding Research*, Gatlinburg, Tenn., pp. 377–381.

16. Adam, G., and Siewert, T. A. 1990. Sensing of GMAW droplet transfer modes using an ER100S-1 electrode. *Welding Journal* 69(3):103-s to 108-s.

17. Lesnewich, A. 1958. Control of melting rate and metal transfer in gas shielded metal arc welding, part II—control of metal transfer. *Welding Journal* 37(4):418-s to 425-s.

18. Deam, R. T. 1989. Weld pool frequency: a new way to define a weld procedure. *Proceedings of the Second International Conference on Trends in Welding Research*, Gatlinburg, Tenn., pp. 967–971.

19. Rohklin, S., Cho, K., and Gun, A. C. 1989. Closed-loop process control of weld penetration using real-time radiography. *Materials Evaluation* 47, pp. 363–369.

20. Smartt, H. B., Einerson, C. J., Watkins, A. D., and Morris, R. A. 1986. Metal arc process sensing and control. *Proceedings of the First International Conference on Trends in Welding Research*, Gatlinburg, Tenn., pp. 461–465.

21. Doumanidis, C. C., and Hardt, D. E. 1989. A model for in-process control of thermal properties during welding. *Trans. ASME, J. Dynamic Systems, Measurements and Control* 111, No. 1.

22. Kim, Y. S., and Eagar, T. W. 1989. Modeling of the temperature distribution in the electrode during GMAW. *Proc. of the Second International Conference on Trends in Welding Research*, Gatlinburg, Tenn., pp. 13–18.

23. Allemand, C. D., Schoeder, R., Ries, D. E., and Eagar, T. W. 1985. Method of filming metal transfer in welding, *Welding Journal* 64(1):45–47.

24. Clark, D. E., 8uhrmaster, C. L., and Smartt, H. B. 1989. Drop transfer mechanisms in GMAW. *Proceedings of the Second International Conference on Trends in Welding Re-*

search, Gatlinburg, Tenn., pp. 371-375.
25. Watkins, A. D. 1989. *Heat Transfer Efficiency in Gas Metal Arc Welding*. M.S. thesis, University of Idaho, Moscow, Idaho.
26. Johnson, J. A., Barna, B. A., Beller, L. S., Taylor, S. C., and Walter, J. B. 1987. A CAMAC-based ultrasonic data-acquisition workstation. *Materials Evaluation* 45, pp. 934-938.
27. Johnson, J. A., Smartt, H. B., Clark, D. E., Carlson, N. M., Watkins, A. D., and Lethcoe, B. J. 1990. The dynamics of droplet formation and detachment in GMAW. Fifth Engineering Foundation Conference on Modeling of Casting, Welding and Solidification Processes, Davos, Switzerland, in press.
28. Johnson, J. A., and Carlson, N. M. 1986. Weld energy reduction by using concurrent nondestructive evaluation. *NDT International* 19, pp. 190-196.
29. Khon, G., and Siewert, T. A. 1987. The effect of power supply response characteristics on droplet transfer of GMA welds. *Proceedings of the ASM International Conference on Trends in Welding Research*, Gatlinburg, Tenn., pp. 299-303.
30. Lancaster, J. F. 1984. Metal transfer and mass flow. J. F. Lancaster, ed. *The Physics of Welding*, International Institute of Welding, Pergamon Press, Oxford, U.K..
31. *Handbook of Chemistry and Physics*, 62nd Edition, 1981, CRC Press, Inc., Boca Raton, Fla., p. F-24.
32. Halmoy, E. 1979. Pulsating Welding Arcs. SINTEF Rapport STF16 A79021.
33. Morris reference to audio signatures of drop transfer.